The Interaction of Human Tryptase-β with Small Molecule Inhibitors Provides New Insights into the Unusual Functional Instability and Quaternary Structure of the Protease†

Trevor Selwood,*,‡ Holly Smolensky,‡ Darrell R. McCaslin,§ and Norman M. Schechter‡

Department of Dermatology, University of Pennsylvania, Philadelphia, Pennsylvania 19104, and Biophysics Instrumentation Facility, Department of Biochemistry, University of Wisconsin, Madison, Wisconsin 53706

Received October 19, 2004; Revised Manuscript Received December 23, 2004

ABSTRACT: Human tryptase-β (HTβ) is a serine protease with an atypical tetrameric structure and an unusual dependence on heparin binding or high salt for functional and structural stability. In the absence of heparin and at physiological salt, pH, and temperature, HTβ rapidly loses activity by a reversible process that we have called spontaneous inactivation. The role of tetramer dissociation in this process is controversial. Using small irreversible or competitive inhibitors of HTβ as stabilizing ligands, we were able to examine tetramer stability under inactivating (decay) conditions in the absence of heparin and to define further the process of spontaneous inactivation. Size exclusion chromatography showed that interaction with inhibitors stabilized the tetramer. Using sedimentation equilibrium, spontaneously inactivated HTβ (si-HTβ) was shown to be a destabilized tetramer that dissociates upon dilution and which in the presence of a competitive inhibitor re-formed a stable tetramer. Addition of inhibitors to si-HTβ rescued catalytic activity as was shown after inhibitor displacement. At high concentrations of si-HTβ (4−5 μM), the binding of inhibitor alone provided sufficient free energy for complete reactivation and tetramer stabilization, whereas at low si-HTβ concentration (0.1 μM) where the destabilized tetramer would be mostly dissociated, reactivation required more free energy which was provided by the binding of both an inhibitor and heparin. The results demonstrate that HTβ is a tetramer in the absence of heparin and that tetramer dissociation is a consequence of and not a prerequisite for inactivation. Heparin binding likely stabilizes the tetramer by favoring a functionally active conformation with stable intersubunit contacts, rather than by simply cross-linking active monomers.

Human tryptase-β (HTβ),[1] the major protein stored within mast cell secretory granules (*1*), is a serine protease that exhibits a number of unusual features. Unlike other serine proteases, it is a tetramer of identical subunits of 27.5 kDa (*2*−*6*). The tetramer is atypical in that the subunits frame a central aqueous pore into which the active sites face, as depicted in Figure 1 (*6*). Two types of interfaces produce the tetramer. One type has a buried surface area of 1100 Å^2 and is structurally symmetric, whereas the other has a smaller surface area of 500 Å^2 and is structurally asymmetric. Two other unusual features of HTβ are its insensitivity to physiological inhibitors (*7*−*9*) and its functional instability (*2*−*5*). The somewhat inaccessible location of the active sites may explain the insensitivity to biological inhibitors, which are macromolecules. Functional instability is manifest as the rapid loss of enzymatic activity ($t_{1/2}$ of about 1 min) when HTβ is incubated under conditions approximating physiological (*4*, *10*). This autoinactivation may substitute for a physiological inhibitor.

We refer to the activity loss process as spontaneous inactivation because it is nonproteolytic and first order (*4*). Its rate is dependent on temperature and NaCl concentration and is markedly reduced by the presence of heparin, a polyanionic glycosaminoglycan coproduced with HTβ in mast cells (*11*, *12*). Activity loss is associated with conformational changes that affect both the CD and intrinsic fluorescence spectra of HTβ (*13*−*15*). Accompanying these conformational changes is the disruption of the primary substrate specificity pocket (S1 pocket) (*15*). Inactivated HTβ can be reactivated by the addition of heparin, demonstrating the reversibility of spontaneous inactivation (*3*, *4*, *16*).

Spontaneous inactivation is accompanied by dissociation of the tetramer (*3*, *5*, *14*, *16*); however, the extent and role of dissociation in activity loss are controversial. Two minimal pathways shown in Figure 1 depict this controversy. In pathway A, the subunits of the tetramer undergo conforma-

† This work was supported by NIH Grant AI45075. Sedimentation equilibrium studies were performed at the University of Wisconsin−Madison Biophysics Instrumentation Facility established by the University of Wisconsin−Madison and Grants BIR-9512577 (NSF) and S10 RR13790 (NIH).

* Corresponding author. Tel: 215-898-0168. Fax: 215-573-2033. E-mail: selwood@mail.med.upenn.edu.

‡ University of Pennsylvania.

§ University of Wisconsin.

[1] Abbreviations: AEBSF, 4-(2-aminoethyl)benzenesulfonyl fluoride; BPTI, bovine pancreatic trypsin inhibitor; BSA, bovine serum albumin; CBZ-GPR-AMC, *N*-carbobenzyloxyglycylprolylargininyl-7-amido-4-methylcoumarin; CD, circular dichroism; DFP, diisopropyl fluorophosphate; FA, fractional activity; HTβ, human tryptase-β; K_i, equilibrium inhibition constant; L-BAPNA, N^{α}-benzoyl-L-arginine *p*-nitroanilide; LBTI, lima bean trypsin inhibitor; MW, molecular weight; NPGB, *p*-nitrophenyl *p*-guanidobenzoate; pAb, *p*-aminobenzamidine; rHTβ, recombinant human tryptase-β; SBTI, soybean trypsin inhibitor; SEC, size exclusion chromatography; si-HTβ, spontaneously inactivated HTβ; si-rHTβ, spontaneously inactivated rHTβ; TOS-GPK-NA, *N*-*p*-tosylglycylprolyllysine *p*-nitroanilide.

10.1021/bi047765u CCC: $30.25
Published on Web 02/12/2005

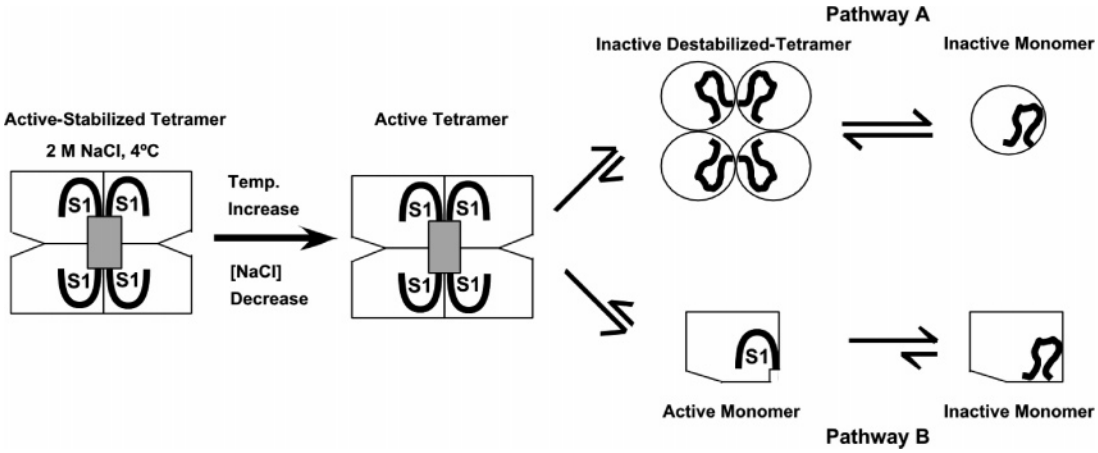

FIGURE 1: Possible pathways (A and B) for the spontaneous inactivation of HTβ. Spontaneous inactivation was initiated by shifting from solution conditions that stabilize activity (e.g., 2.0 M NaCl, 4 °C, pH 6.8) to conditions where activity is rapidly lost (e.g., 0.2 M NaCl, 37 °C, pH 6.8). The primary specificity (S1) pocket, which binds the Lys/Arg residue on the N-terminal side of the scissile bond in substrates, is open to depict the active conformation and closed to depict loss of function. In pathway A, destabilization of the tetramer is depicted by a change from square-like to circular subunits, and in pathway B the interface change is depicted as small and only in the region of the S1 pocket. The gray area depicts the central aqueous pore of the active tetramer.

tional changes that result in both activity loss and tetramer destabilization. Evidence for pathway A is derived from sedimentation equilibrium analyses showing that HTβ when stabilized in high salt is a homogeneous tetramer, while under similar conditions si-HTβ exists as an equilibrium mixture of tetramer and monomer (*14*). Additional support is derived from the stability of rHTα, a protein 93% identical in amino acid sequence to HTβ. Although exhibiting a similar quaternary structure (*17*), rHTα does not dissociate upon prolonged incubation under decay conditions (*18*). The crystal structures of HTβ and rHTα were similar except for the conformation of their S1 pockets (*6*, *17*).

In pathway B, the tetramer is a loose aggregate of monomers held together by weak contacts that are enhanced by high salt or by heparin cross-linking of monomers. In the aggregated state, contacts between adjacent monomers stabilize the S1 pocket. Lowering the salt concentration or dissociation of heparin results in rapid tetramer dissociation followed by an isomerization that disrupts the S1 pocket. In support of pathway B is the unusual tetramer structure and implied weakness of the small interface (*6*), a study suggesting that the appearance of the inactive tetramer occurs after the production of inactive monomer (*5*), and studies indicating that heparin stabilization is mediated by the cross-linking of monomers via binding across the small interface (*19*, *20*). A heparin-stabilized HTβ monomer with enzymatic activity (*3*, *21*, *22*) and sensitivity toward protein proteolytic inhibitors (*21*, *22*) also has been reported. Whether this monomer is formed simply by dissociation of the heparin-stabilized tetramer is unclear.

To understand the stability of the tetramer under decay conditions and to distinguish between pathways A and B, the quaternary structure of HTβ and the reactivation of si-HTβ were investigated utilizing small molecule inhibitors as stabilizing ligands. These inhibitors bind only to the active site, predominately the S1 pocket, and therefore would be expected to stabilize HTβ in its active conformation under decay conditions without cross-linking. Pathway A posits HTβ and reactivated si-HTβ would be stabilized as a tetramer, whereas pathway B posits dissociation to monomers. Our results find that pathway A best accounts for the structure of active HTβ, the mechanism of spontaneous inactivation, and tetramer dissociation.

EXPERIMENTAL PROCEDURES

Materials. LMW heparin, AEBSF, and buffers were from Calbiochem, La Jolla, CA. The chromogenic substrates L-BAPNA and TOS-GPK-NA, bovine serum albumin, LBTI, and BPTI (aprotinin) were from Sigma, St. Louis, MO. The fluorescent substrate CBZ-GPR-AMC and the inhibitor pAb were from Bachem, King of Prussia, PA. Leupeptin (Ac-Leu-Leu-argininal) was from Roche, Indianapolis, IN. CRA-2059 was a gift from Celera Genomics, Inc.

rHTβ. rHTβ referred to in the text is our rHT-βII variant, rHTβ-E149T described previously (*18*, *23*). The variant has comparable stability and catalytic properties to wild-type rHTβ and to native tryptase isolated from human skin. The mutation eliminates a site within rHTβ sensitive to the protease that processes our fusion protein construct. Stock enzyme was stored at −70 °C in 2.0 M NaCl and 10 mM MOPS, pH 6.8, until needed. Preparations were >90% active based on concentrations determined using previously established specific activities for substrates compared to concentrations estimated using A_{280nm} [ϵ(HTβ_{280nm}) = 64900 M^{-1} cm^{-1}] (*18*). Concentrations reported are those of the active subunit, except in sedimentation equilibrium studies where subunit concentration was based on A_{280nm}. The concentrations of si-rHTβ were based on the active subunit concentration of an identical amount of stock rHTβ diluted into decay buffer containing 0.5 mg/mL heparin.

Measurement of Hydrolytic Activity. Assays were performed in a 1 cm path length cuvette using either L-BAPNA (1 mM), TOS-GPK-NA (1 mM), or CBZ-GPR-AMC (35 μM) in 0.2 M NaCl, 0.1 M Tris-HCl (pH 8.0), 0.1 mg/mL heparin, and 9% Me_2SO, at 25 °C. These assay conditions do not produce loss/gain of activity. The substrate concentrations are well below the K_M (*18*). The presence of heparin stabilizes active rHTβ but does not mediate reactivation at the protease concentration (0.1−80 nM) and pH (*16*) of the assay. Enzymatic activities reported are initial velocities measured over a 3 min period by monitoring either NA accumulation at A_{410nm} in a Beckman DU 640 spectropho-

tometer or AMC accumulation by fluorescence emission (ex/em 370/475 nm) in a Photon Technologies International QM C60 fluorometer. In all measurements <10% of the substrate was consumed, and product accumulation was linear.

Assays with L-BAPNA were used to monitor the hydrolytic activity of aliquots removed from decay/reactivation mixtures containing ≥4.0 μM rHTβ/si-rHTβ; the dilution was 50-fold into assay medium. TOS-GPK-NA was used to monitor activity of aliquots removed from inhibitor-mediated reactivations containing ≥4.0 μM si-rHTβ; the dilution was 1000-fold. CBZ-GPR-AMC was used to monitor activity of aliquots removed from decays/reactivations of 0.1 μM rHTβ/si-HTβ; the dilution was 1000-fold.

Inhibitors. The stock concentrations of leupeptin (10 mM in 0.01 M MOPS, pH 6.8), BPTI (10 μM in water), and LBTI (80 μM in water) were determined by titration with bovine trypsin previously standardized with NPGB (*4*). The stock concentration of pAb (200 mM in 1.0 M MOPS, pH 6.8) was determined by absorbance assuming ϵ_{293nm}(pAb) = 15000 M^{-1} cm^{-1} (*24*). The stock concentrations of AEBSF (5 mM in water) and CRA-2059 (30 mM in Me_2SO) were based on weight.

The K_i values for the interaction of leupeptin and pAb with 6 nM rHTβ stabilized by heparin were determined at 25 °C in 0.2 M NaCl, 10 mM MOPS (pH 6.8), 9% Me_2SO, and 0.5 mg/mL heparin and with the [inhibitor] ≫ [rHTβ]. Buffer, inhibitor, and rHTβ were mixed in a cuvette to a reaction volume of 450 μL. Activity remaining was then measured after addition of 50 μL of 10 mM TOS-GPK-NA. As noted above, 1 mM substrate is ≪K_M. Thus, the small dilution and substrate addition did not perturb the binding equilibrium significantly. Reactions with leupeptin were incubated for 15 min before substrate addition to allow for the relatively slow dehydration of the aldehyde hydrate (*25*). Reactions with pAb were assayed after a 2.0 min incubation. Fraction inhibited vs $[I]_0$ plots were hyperbolic, and K_i values were determined by fitting the data to eq 1, where fraction inhibited = 1 − [(activity with inhibitor)/(activity without inhibitor)].

$$\text{fraction inhibited or returned} = [I]_0/(K_i + [I]_0) \quad (1)$$

Spontaneous Inactivation/Reactivation of rHTβ. Decays were initiated by a ≥10-fold dilution of rHTβ stock solution into buffer to give conditions of 0.2 M NaCl and 10 mM MOPS, pH 6.8, at 30 or 37 °C. Dodecyl maltoside (final concentration, 0.1%) was added to inactivations/reactivations of 0.1 μM rHTβ to limit nonspecific loss of the protease. FA is the (activity of sample)/(activity of the control at time 0), where the control was stabilized by 0.5 mg/mL heparin.

The si-rHTβ used in reactivations was produced by decay of 0.1, 4.0, or 8.0 μM rHTβ at 30 or 37 °C for 0.5 h when FA was <0.04. The si-rHTβ solution was adjusted to 25 °C, and reactivation was initiated by addition of inhibitors and/or 0.5 mg/mL heparin. These additions produced ≤10% dilution of si-rHTβ. Reactivations were monitored periodically for a total time of 4−5 h, until activity no longer increased; the slowest reactivations were at low inhibitor concentration. In reactions with competitive inhibitors dilution into assay medium resulted in displacement of the inhibitor while heparin functioned to stabilize the reactivated protease, thereby permitting measurement of hydrolytic activity. Because the dilution was not sufficient to completely dissociate the inhibitor from rHTβ at high inhibitor concentrations, fraction returned was determined by comparison to a parallel control with the same inhibitor and rHTβ concentration but stabilized by 0.5 mg/mL heparin. This control was diluted and assayed identically to the reactivation sample and thus provided an estimate of the maximum activity at each concentration of inhibitor. BSA (1.0 mg/mL) was included with leupeptin to limit possible irreversible inactivation of rHTβ by the reaction of the aldehyde group with free amino groups of si-rHTβ. This inclusion increased the extent of the returns at high leupeptin concentrations. The dissociation of rHTβ−leupeptin complexes was slow; therefore, steady-state rates were taken 15 min after dilution when product accumulation was linear.

Susceptibility to the inhibitor CRA-2059 was used to indicate the aggregation state of si-rHTβ which was reactivated at low concentration. CRA-2059 is a bivalent inhibitor composed of two phenylguanidinium headgroups joined by a synthetic linker (*10*). It interacts with the S1 pockets of two adjacent rHTβ subunits producing a K_i value of 0.6 nM (*10*). The K_i is approximately 10^4-fold higher for partially modified AEBSF−rHTβ tetramers with a single unmodified subunit (*10*), indicating that the inhibitor would bind much more weakly to an active tryptase monomer. Although a tight binding inhibitor of the active tetramer, CRA-2059 does not reactivate si-rHTβ (unpublished observation) for reasons that are as yet unclear. Given these properties, 30 nM CRA-2059 could only inhibit the tetrameric form of HTβ. To determine if 0.1 μM si-rHTβ reactivated by heparin or heparin plus pAb was sensitive to 30 nM CRA-2059, reactivated enzyme was diluted to 0.1 nM in a 1 mL cuvette. After activity was measured using the fluorescent substrate, 1.0 μL of 30 μM CRA-2059 was added. Immediate inhibition of activity was taken as indicative of the tetrameric state. Inhibition of a dimeric form of rHTβ cannot be eliminated, although no evidence for a stable dimer exists at present.

AEBSF Modification of rHTβ. To completely modify (inhibit) rHTβ, 2 μL of 30 mM AEBSF was added to 70 μL of 100 μM rHTβ in 2.0 M NaCl and 10 mM MOPS, pH 6.8 at 25 °C. Inhibition was monitored using L-BAPNA until over 98% of the starting activity was lost ($t_{1/2}$ = 10 min). Partially modified preparations of rHTβ (57% and 82% inhibited) were prepared by the same protocol except that the AEBSF concentration was substoichiometric (*10*). The distribution of tetrameric species with zero, one, two, three, and four modified subunits was calculated assuming random modification using eq 2, where $P(N)$ is the probability for a tetramer with N number of modified subunits and M is the fraction of the initial activity lost by modification.

$$P(N) = M^N(1 - M)^{(4-N)}(4!/(N!(4 - N)!)) \quad (2)$$

Size Exclusion Chromatography. Analyses were performed using a Superose-12 HR 10/30 FPLC column equilibrated at 25 °C in 2.0 or 0.2 M NaCl and 0.01 M MOPS (pH 6.8). All samples were loaded in 0.1 mL of the low-salt buffer and eluted with either high- or low-salt buffer at a flow rate of 0.5 mL/min. Elution was monitored continuously at A_{230nm} and A_{280nm} using a Perkin-Elmer LC-235 diode array detector. To mark the total volume of each analysis, 10 μL of 1.0 M MOPS (pH 6.8) was added to each sample before loading

unless otherwise stated. MOPS absorbs at 230 nm, and its elution time was 34 min. Other calibration markers were DNA (void volume), IgG (150 kDa), α-1-antichymotrypsin (45 kDa), and chymotrypsinogen (23.5 kDa). The total protein loaded onto the column was determined from the A_{230nm} of the sample in a spectrophotometer before MOPS addition. This value was compared to the integrated A_{230nm} elution profile recorded by the column detector to provide an estimate of the amount of protein recovered. A conversion factor between detector and spectrophotometer-based A_{230nm} was established in an experiment where fractions were collected, and the sum of the A_{230nm} of fractions measured in a spectrophotometer was related to the integrated A_{230nm} from the detector. Inhibitors eluted later than MOPS, presumably due to nonspecific interaction with the matrix. In high salt AEBSF and leupeptin eluted at 75 and 42 min, respectively, and in low salt they eluted at 54 and 36 min, respectively.

Sedimentation Equilibrium. To produce si-rHTβ, rHTβ in 2 M NaCl was diluted to 0.2 M NaCl and 10 mM MOPS, pH 6.8, and the activity was allowed to decay at room temperature for 1.5−3 h. For the stabilized control, rHTβ was diluted using 2 M NaCl and subjected to the same room temperature incubation. At the end of the incubation period, leupeptin was added to the si-rHTβ to give the final concentrations 0.9, 0.5, and 0.05 mM; leupeptin also was added to the control. The final concentrations of rHTβ were based on the A_{280nm} measured in the centrifuge using a 1.2 cm path length.

Sedimentation equilibrium experiments were performed at 4 °C and at several speeds in a Beckman XL-A analytical ultracentrifuge. Approximately 100 μL of each sample was loaded into cells with 1.2 cm double sector charcoal-filled epon centerpieces; the reference was 105 μL of the appropriate buffer without leupeptin. Gradients were monitored until they became superimposable when recorded 3 or more hours apart. In studies using BPTI, gradients were recorded at A_{290nm} as well as A_{280nm}. At the former wavelength, the contribution from BPTI is negligible due to the lack of Trp residues. The buffer densities of 1.017 g/mL (0.2 M NaCl) and 1.077 g/mL (2 M NaCl) were measured at 4 °C in an Anton Parr DMA5000 density meter. The partial specific volumes for rHTβ (27.5 kDa) and a 1:1 complex with BPTI (complex = 33.9 kDa) were calculated from sequence data as 0.735 and 0.731 mL/g, respectively

Weight-average MWs were determined over a range of data using linear regression to approximate the slopes of tangents to the curves. When curvature of the plot was obvious, data were evaluated over limited ranges at low and high radial positions; otherwise, the complete data set was used. The concentrations reported are based on the mean of the ln *A* data included in the regression.

Data Analysis. Data were analyzed by linear or nonlinear least squares regression using Igor Pro (Wavemetrics, Lake Oswego, OR). Errors are standard deviations obtained from the curve fits. Data analysis and presentation of sedimentation equilibrium data used software developed in IGOR Pro by Darrell R. McCaslin.

RESULTS

A Small Irreversible Inhibitor Stabilizes the Tetramer. AEBSF is an irreversible inhibitor of trypsin-like proteases

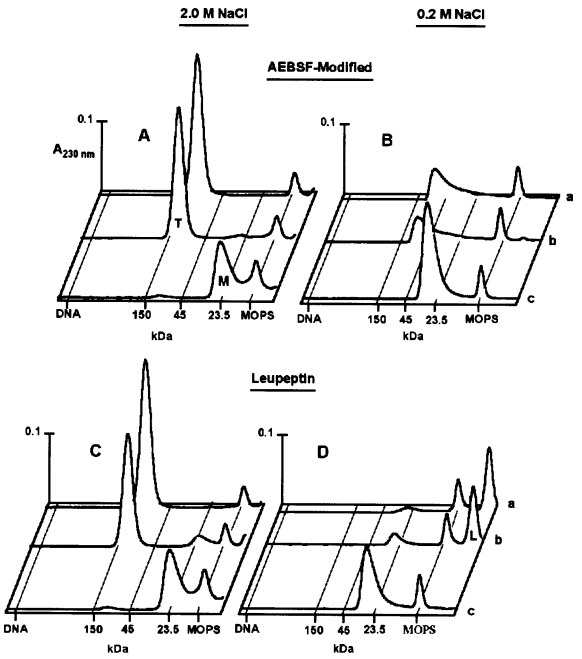

FIGURE 2: SEC of inhibitor stabilized rHTβ, reactivated rHTβ, and si-rHTβ. In all analyses, 0.1 mL of 5.0 μM (125 μg) protease ± inhibitor was loaded into the injector in decay buffer (0.2 M NaCl, pH 6.8). Protease was eluted at 25 °C with low- or high-salt buffer and A_{230nm} monitored. Weights shown on the *x*-axis mark the elution of calibration proteins and the total volume marker, MOPS. The elution of inactive monomer (27.5 kDa) and active rHTβ tetramer (110 kDa) is indicated as M and T, respectively. Panels A and B show the elution patterns for AEBSF-modified rHTβ as follows: traces a, AEBSF-modified rHTβ immediately after dilution into decay buffer at 37 °C; traces b, AEBSF-modified rHTβ after 24 h incubation in decay buffer at 37 °C; traces c, unmodified rHTβ after 30 min in decay buffer at 37 °C. Panels C and D show the elution patterns for rHTβ incubated with leupeptin as follows: traces a, rHTβ incubated with 1 mM leupeptin; traces b, si-rHTβ reactivated by 1 mM leupeptin; traces c, si-rHTβ after 30 min of decay at 37 °C. The elution buffer for traces a and b of panel D contained 1 μM leupeptin. Excess leupeptin in the sample eluted slightly after the MOPS peak in the low-salt analyses (marked L) of panel D and much later than the MOPS peak in the high-salt analyses of panel C (peak not shown).

(*10*, *26*−*28*), which binds to the S1 pocket and chemically modifies Ser195 [all numbering is by alignment with chymotrypsinogen (*18*)]. SEC was used to examine the quaternary structure of unmodified and AEBSF-modified rHTβ after incubation in decay buffer at 37 °C where the half-life for decay of unmodified rHTβ is about 1 min (*18*). rHTβ was completely modified with AEBSF while stabilized in high-salt solution. Both modified and unmodified stock solutions were diluted 20-fold into decay buffer to initiate incubations, and aliquots of equal protein content were loaded onto the SEC column which was then developed with high-salt (Figure 2A) and low-salt (Figure 2B) elution buffers.

AEBSF-modified rHTβ immediately after dilution and after 24 h of incubation under decay conditions showed little, if any, change in elution profile (traces a and b, respectively). The major peak under both salt conditions eluted as a large protein of 100 kDa. In contrast, after 30 min of decay unmodified rHTβ eluted as a monomer at 25 kDa (traces c). The different elution patterns suggested that modification prevented spontaneous inactivation and stabilized the tetramer.

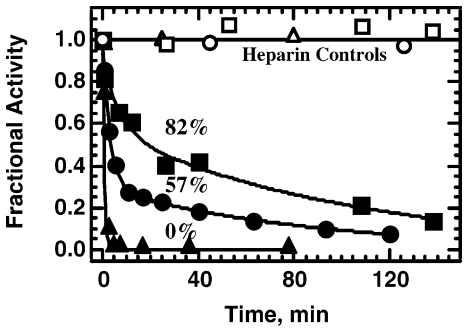

FIGURE 3: Time courses for inactivation of rHTβ modified with substoichiometric concentrations of AEBSF. Decay conditions were 0.2 M NaCl, pH 6.8, and 37 °C. Each of the decays contained 5 μM rHTβ subunits where 0% (filled triangles), 57% (filled circles), or 82% (filled squares) of the subunits had been modified by AEBSF. The solid lines are fits of the data to a sum of two exponentials; parameters are described in the text. Corresponding open symbols are parallel incubations containing 0.5 mg/mL heparin as a stabilizer.

Creating some ambiguity in the results was the shape of high MW peaks and the amounts of AEBSF-modified rHTβ recovered in the different elution buffers. High-salt elution profiles showed well-defined tetramer peaks that accounted for nearly 100% of the protein loaded (Figure 2A, traces a and b), whereas low-salt elution profiles exhibited a much broader peak that eluted at a slightly lower MW position than the high-salt tetramer and corresponded to about 50% of the protein loaded (Figure 2B, traces a and b). The loss of protein is probably not due to dissociation of the tetramer, as unmodified si-rHTβ is recovered as monomer in both high- and low-salt elutions. The slightly later elution position of the high MW peak in low salt may suggest the dissociation of the tetramer. However, as will be shown later in studies with leupeptin, the most likely explanation for the appearance of the low-salt elution profiles is the nonspecific interaction of tetramers with the column matrix.

Tetramer integrity under decay conditions was further analyzed by characterizing the rate of spontaneous inactivation of rHTβ partially inhibited by AEBSF. At substoichiometric levels of modification, rHTβ tetramers will be a mixture containing 0−4 modified subunits/tetramer with the distribution being a function of the extent of modification (eq 2). If activity loss and tetramer integrity are linked as in pathway A, the juxtaposition of AEBSF-modified subunits to unmodified subunits should add stability to the unmodified subunits. Alternatively, if the tetramer is a loose aggregate of monomers as in pathway B, AEBSF modification should have little, if any, effect on the rate of activity loss of unmodified subunits.

In Figure 3 are shown the time courses of spontaneous inactivation for 0%, 57%, and 82% modified rHTβ. Both modified preparations decayed more slowly than the unmodified ($t_{1/2}$ at 37 °C of 1 min), and each required two exponential processes to describe their time course of activity loss (solid lines in Figure 3). The half-life values for activity loss of 57% modified rHTβ were 90 and 2.2 min with relative contributions of 30% and 70%, respectively, and for 82% modified rHTβ they were 70 and 3.5 min with relative contributions of 60% and 40%, respectively. The markedly slower decay rates of tetramers with mixtures of modified and unmodified subunits imply that intersubunit contacts play a role in stabilizing the tetramer.

The biphasic nature of the decays appears rooted in the various combinations of unmodified and modified subunits within the tetramer. When either three subunits or two diagonally located subunits are modified, then the large and small interfaces of the remaining unmodified subunits are both formed with modified subunits and give rise to the slower decaying population. On the other hand, when one subunit or two adjacent subunits are modified, the unmodified subunits will either not be in contact with a modified subunit or be in contact at only one interface. This latter population along with tetramers containing no modified subunits would form the faster decaying population. The predicted ratios based on eq 2 for the more:less stable populations are 33:67 for 57% modified rHTβ and 54:46 for 82% modified rHTβ. These ratios qualitatively mirror the relative contributions of the slow and fast phases described above.

The effect of complete modification on tetramer stabilization, and partial modification on the rate of activity loss, suggests that activity loss is linked to conformational changes at both subunit interfaces. This finding supports pathway A where the product of spontaneous inactivation is an inactive destabilized tetramer.

Reactivation of rHTβ Mediated by Small Reversible Inhibitors. To determine if small molecule inhibitors were capable of reactivating si-rHTβ, the interactions of the competitive inhibitors pAb and leupeptin with si-rHTβ were investigated. In these studies, 4−5 μM rHTβ was spontaneously inactivated under decay conditions at 30 °C. The reaction mixture was then divided into 50 μL aliquots and cooled to 25 °C before varying amounts of inhibitor were added. The extent of reactivation at 25 °C was determined after a large dilution into the standard assay. The dilution served to dissociate inhibitor bound to reactivated protease. To estimate fraction returned, recovered activity was compared to that of a heparin-stabilized rHTβ control that was treated with inhibitor and diluted in a parallel manner.

Both leupeptin and pAb mediated the reactivation of si-rHTβ in a concentration-dependent manner. In Figure 4, the concentration dependence for each inhibitor to reactivate si-rHTβ is compared to that for each to inhibit heparin-stabilized rHTβ. Both inhibition and reactivation data were fit well by the simple mass action binding model of eq 1. The K_i's for the inhibition of rHTβ (Figure 4, circles) were 1.0 and 65 μM for leupeptin and pAb, respectively, while the corresponding apparent K_i's for the reactivation of si-rHTβ (Figure 4, squares) were 100 μM and 4 mM. The displacement of the reactivation curves to higher concentrations than the inhibition curves ($\Delta K_i = 50-100$ at 25 °C) is consistent with the loss of 2−3 kcal/mol of favorable free energy in the binding of either leupeptin or pAb to si-rHTβ relative to heparin-stabilized rHTβ. This difference in free energy, which is independent of the choice of inhibitor, must correspond to that needed for reorganization to the active structure.

SEC was used to analyze 5.0 μM rHTβ treated with 1.0 mM leupeptin (Figure 2C,D, traces a) or 5.0 μM si-rHTβ completely reactivated by 1 mM leupeptin (Figure 2C,D, traces b). Both rHTβ and si-rHTβ treated with leupeptin eluted as tetramers in high salt with almost complete recovery of protein, which is consistent with the reactivation of si-rHTβ as determined by activity. Parallel analyses in low salt (Figure 2D, traces a and b) showed extensive loss of protein,

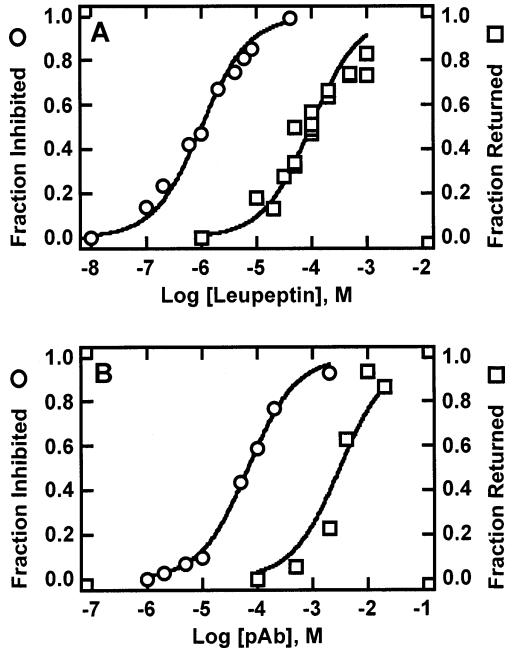

FIGURE 4: Interaction of leupeptin and pAb with heparin-stabilized rHTβ and si-rHTβ. The inhibition of heparin-stabilized rHTβ (circles) by either leupeptin (panel A) or pAb (panel B) is compared to the extent of reactivation (squares) mediated by these inhibitors. Inhibition and reactivation studies were performed in 0.2 M NaCl, pH 6.8, at 25 °C. The extent of reactivation was assumed to equate with the ability of si-rHTβ to bind inhibitor; therefore, both fraction inhibited and fraction returned should reflect the formation of the inhibitor−rHTβ complex. The concentration of heparin-stabilized rHTβ in inhibition studies was 6.0 nM, and the concentration of si-HTβ in reactivations was between 4 and 6 μM. Inhibitor concentrations were in excess of HTβ and si-HTβ concentrations; thus x-axis $\approx$ free inhibitor. K_i values were determined from the data assuming eq 1. Both data and fits to eq 1 were transposed to a log scale for presentation.

and thus, the ability of leupeptin to stabilize the rHTβ tetramer in decay buffer and to mediate reassembly of the tetramer from si-rHTβ could not be established by SEC. The loss of protein seemed to be a more extreme case of the behavior observed with AEBSF-modified rHTβ. Below, sedimentation equilibrium is used to demonstrate the ability of leupeptin to stabilize the tetramer, indicating that the poor recoveries of inhibitor−rHTβ complexes in low-salt elutions were likely due to nonspecific adsorption to the gel matrix.

Interaction of si-rHTβ with Leupeptin Characterized by Sedimentation Equilibrium. Sedimentation equilibrium measures the weight-average MW of a protein from its distribution in a centrifugal field. Representative examples of sedimentation equilibrium data for rHTβ stabilized in high salt with leupeptin and si-rHTβ in decay buffer (4 °C) with and without leupeptin are shown in Figure 5A,B. Data are plotted as the natural logarithm of protein concentration (as indicated by A_{280nm}) vs radial position squared (r^2); the slope at any r^2 is directly proportional to the weight-average MW at that position. For rHTβ stabilized with high salt plus leupeptin, plots were linear at all speeds, demonstrating the presence of a single species (e.g., Figure 5A, open triangles) with a MW approximately equal to that of the tetramer. In contrast, plots of si-rHTβ in 0.2 M NaCl without leupeptin were curved upward at most speeds (e.g., Figure 5A, open boxes). Such curvature indicates that the weight-average MW is a function of the protein concentration. A representative

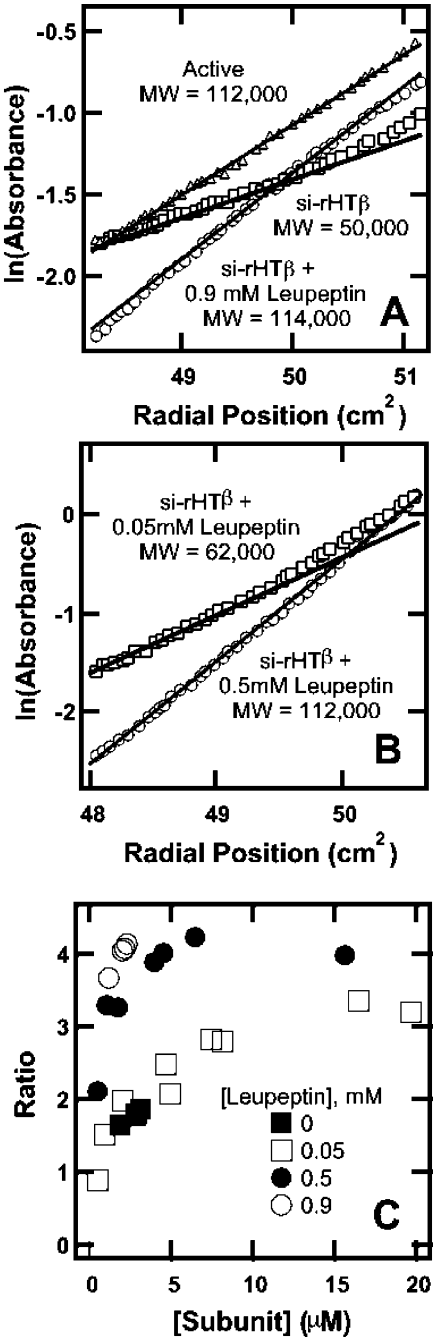

FIGURE 5: Sedimentation equilibrium studies of si-rHTβ with leupeptin. Data at various speeds were obtained at 4 °C, and protein concentration was measured by A_{280nm}. For clarity of the presentation only every third data point is shown. The buffer was 0.2 M NaCl, 10 mM MOPS, pH 6.8, except for the analysis of stabilized rHTβ which was performed in 2.0 M NaCl, 10 mM MOPS, pH 6.8. In panel A the speed was 8800 rpm. Triangles are for 3.8 μM active rHTβ (at loading) in 2.0 M NaCl with 0.9 mM leupeptin. Squares are for 3.4 μM si-rHTβ in the absence of leupeptin, and circles are for 3.2 μM si-rHTβ with 0.9 mM leupeptin. For panel B the speed was 12400 rpm, and the data are for 7.7 μM si-rHTβ with 0.05 mM (squares) or 0.5 mM (circles) leupeptin. Weight-average molecular weights were calculated by linear regression as described in the text. In panel C, the sedimentation equilibrium data for si-rHTβ are presented as the ratio of the weight-average molecular weight to the subunit molecular weight, plotted as a function of the subunit concentration at the measurement position, and include measurements at speeds in addition to those shown in panels A and B.

weight-average MW calculated from a tangent at small radial position (low protein concentration) shown in Figure 5A is greater than that of monomer and, therefore, indicates a mixture of species. The maximum MW based on tangents at large radial position (higher concentration) was indicative of the presence of some tetrameric species. These results are consistent with a previous sedimentation equilibrium study performed in 1.0 M NaCl with HTβ purified from human skin where the concentration dependence of the MW was best described as an equilibrium between monomer and tetramer species (*14*).

The effect of leupeptin concentration on the weight-average MW of si-rHTβ in 0.2 M NaCl is illustrated in Figure 5A,B. Leupeptin was added to si-rHTβ samples produced by decay before centrifugation. At all speeds, si-rHTβ in 0.9 mM leupeptin was a homogeneous population of tetramers (e.g., Figure 5A, open circles), indicating that the position of the monomer/tetramer equilibrium had markedly shifted to the tetramer. The shift to tetramer was not as complete at the lower leupeptin concentrations. A mixture of species was still obvious at some speeds, as illustrated by the curvature in the plot for 0.05 mM leupeptin (Figure 5B, open squares). Although leupeptin was always in molar excess of si-rHTβ, the curvature suggests that its concentration was not high enough to drive the equilibrium to tetramer at all protein concentrations reached in the gradients. The effect of leupeptin and protein concentration on the weight-average MW of si-rHTβ is summarized in Figure 5C. The results are presented as the measured weight-average MW calculated at various r^2 in the cell divided by the polypeptide MW (27.5 kDa) plotted against the total subunit concentration at the r^2 used for the calculation. Clearly, the weight-average MW of si-rHTβ−leupeptin mixtures is a function of both protein and inhibitor concentrations, where increasing either shifts the population toward the tetrameric form.

These sedimentation equilibrium studies show that addition of leupeptin, a small competitive inhibitor of rHTβ, can drive si-rHTβ completely to tetramer, even under inactivating conditions (0.2 M NaCl) where si-rHTβ is partially monomeric (Figure 5C). The same high concentration of leupeptin (1.0 mM) that produced the complete return of enzymatic activity in reactivations (Figure 4A) also converted si-rHTβ to a virtually homogeneous population of tetramers, demonstrating that the return of enzymatic activity in reactivations was associated with reassembly of the active tetramer. Lower leupeptin concentrations, which produced less return of enzymatic activity in reactivations, also produced less extensive conversion of si-rHTβ to the tetrameric state, adding further support to the linkage between the tetrameric state and activity. These results support pathway A by showing that si-rHTβ is a mixture of different molecular weight species in equilibrium and that the tetramer is the favored structure of the active protease even in decay conditions.

Reactivation of si-rHTβ at Low Concentration. It has been reported that reactivation of si-rHTβ by heparin is a pH-dependent process that only occurs below pH 6.5 (*16*, *22*). At pH 6.8, we find little reactivation by heparin of 0.1 μM si-rHTβ but nearly complete reactivation of 4.0 μM si-rHTβ (*4*, *15*). On the basis of the equilibrium association constant (K_A) of 5×10^{15} M^{-3} for si-HTβ determined previously (*14*),

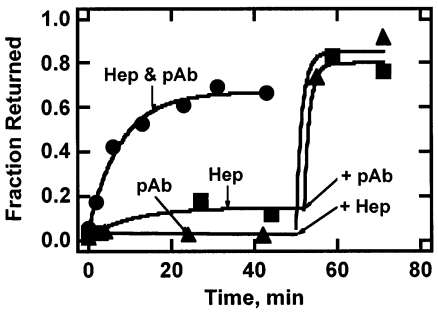

FIGURE 6: Effects of heparin (Hep) and pAb on the reactivation of low concentration si-rHTβ. Reactivation of 0.1 μM si-rHTβ was performed by simultaneous addition of stock pAb and heparin to give 20 mM and 0.5 mg/mL pAb and heparin, respectively (circles). For one case (triangles), addition of pAb was followed after 50 min by heparin, and in another (squares), the sequence was reversed. Reactivation conditions were 0.2 M NaCl, 10 mM MOPS, pH 6.8, and 25 °C. Fractional return was calculated relative to a control as described in Experimental Procedures.

si-rHTβ is about 70% monomeric at 4 μM subunit concentration and virtually completely dissociated at 0.1 μM (see also Figure 5C), indicating a greater free energy requirement for reassembly of the active tetramer at low concentration. To overcome this proposed greater free energy requirement, reactivation of si-rHTβ by heparin was augmented by the addition of pAb, an inhibitor that binds only to the S1 pocket.

As shown in Figure 6, 20 mM pAb alone or 0.5 mg/mL heparin alone produced minimal reactivation of 0.1 μM si-rHTβ after 50 min of incubation. With both heparin and pAb present, the extent of return at low concentration markedly increased to >70% of the predecay level. The extent of return was independent of the addition order, as pAb and heparin added in either order nearly an hour apart produced the same level of return as when added simultaneously. The greater extent of reactivation is consistent with separate binding sites for pAb and heparin and with the free energy available from binding either ligand alone not being sufficient to completely re-form the active tetramer from low concentration si-rHTβ. Given the reported return of low concentration si-rHTβ by heparin alone at pH 6.0 (*16*, *22*), this result confirms that monomeric si-rHTβ is not a dead species in our system and that reactivation is a protein concentration as well as a pH-dependent process. The protein concentration dependence is consistent with pathway A.

SEC could not be used to demonstrate the return of the tetramer because the A_{230nm} of 0.1 μM si-rHTβ was below the detection limits of the column monitor. As described in Experimental Procedures, an alternative method to probe the aggregation state of 0.1 μM reactivated si-rHTβ was devised using CRA-2059, a bivalent inhibitor that binds tightly only to the rHTβ tetramer and does not reactivate si-rHTβ. To maintain an excess of CRA-2059 over enzyme at an inhibitor concentration (30 nM) where only tetramer is reactive, reactivations were diluted to 0.1 nM in assay buffer before addition of inhibitor. Under these conditions, CRA-2059 was shown to inhibit 0.1 μM si-rHTβ that had been reactivated by heparin alone (20% rescue) or by heparin in combination with pAb (70% rescue), suggesting strongly that active tetramer was reassembled in both reactivations.

Trapping of Monomeric si-rHTβ by BPTI. Recently, two laboratories have reported the dissociation of heparin-stabilized HTβ to a monomeric species reactive with BPTI

(*21*, *22*), a protein protease inhibitor (6.5 kDa) that binds tightly to trypsin ($K_i = 10^{-12}$ M) and other monomeric trypsin-like proteases (*29*−*32*). Given the above observations, incubation of heparin-stabilized rHTβ with a high concentration of BPTI would be expected to drive dissociation of the tetramer to inactive BPTI−monomer complexes. In our hands, incubation of 0.5 μM rHTβ stabilized with 0.025 mg/mL heparin showed no loss of activity when incubated with 10.0 μM BPTI for over 24 h under conditions (0.14 mM NaCl, 2.7 mM KCl, 0.01 M phosphate, pH 7.4, 37 °C) reported to favor dissociation (*21*). In addition, 8.0 μM si-rHTβ reactivated by heparin was not sensitive to BPTI as shown in Figure 7A nor was 0.1 μM si-HTβ reactivated by pAb and heparin. In the latter case, BPTI (10.0 μM final concentration) was added to reactivated si-rHTβ after dilution to 0.1 nM to dissociate bound pAb. Thus, we find little, if any, tendency for BPTI to inhibit heparin-stabilized rHTβ.

To determine if BPTI could bind to si-rHTβ, the effect of BPTI on the reactivation of 8.0 μM si-rHTβ by heparin was examined. The addition of BPTI to si-rHTβ before, but not after, the addition of heparin completely prevented reactivation (Figure 7A, triangles), indicating an interaction between BPTI and si-rHTβ. SEC analyses of this reactivation mixture (Figure 7B, trace a) showed a major protein peak corresponding to monomeric si-rHTβ (Figure 7B, trace c). However, comparison of this trace with that of BPTI alone at the same concentration used in the reactivation (dotted trace) revealed a reduced BPTI peak. This reduction implies that the major peak in trace a was that of a monomer−BPTI complex and that the size of BPTI was too small to change the elution position of the peak. Trace b in Figure 7B is a control where BPTI was added to heparin-stablilized rHTβ before chromatography. The elution pattern shows BPTI completely recovered as free BPTI and rHTβ migrating as the tetramer, consistent with the inability of BPTI to interact with and dissociate the stabilized rHTβ tetramer. The minor peak at the total volume position of trace c is MOPS, which was included as the total volume marker in the si-rHTβ alone analysis but not in the other analyses.

Sedimentation equilibrium also was used to establish the interaction of BPTI with si-rHTβ (Figure 7C). Analyses were in decay buffer (4 °C) containing 4.5 μM si-rHTβ with and without 10 μM BPTI. The BPTI-containing sample appeared as a single species at all speeds (Figure 7C) with a MW of 36500, in good agreement with the expected value of 33865 calculated for a 1:1 monomer−BPTI complex. The weight was lower than that of si-rHTβ, which is the weight-average MW of a mixture of monomers and tetramers. The reduction in weight demonstrates further the interconvertibility of all species comprising si-rHTβ, with leupeptin driving all to tetramer and BPTI dissociating all species to produce a BPTI−monomer complex.

To determine if si-rHTβ is generally susceptible to protein proteolytic inhibitors, a similar study was performed using LBTI instead of BPTI. LBTI is a two-headed protein inhibitor (10 kDa) in which at least one head binds strongly to trypsin-like proteases (*33*). The effect of LBTI on reactivation by heparin was not as dramatic (Figure 7A, squares) as that of BPTI (Figure 7A, triangles). LBTI decreased the rate, but not the extent, of reactivation, suggesting a weak interaction that could not prevent the return of si-rHTβ to the active tetramer.

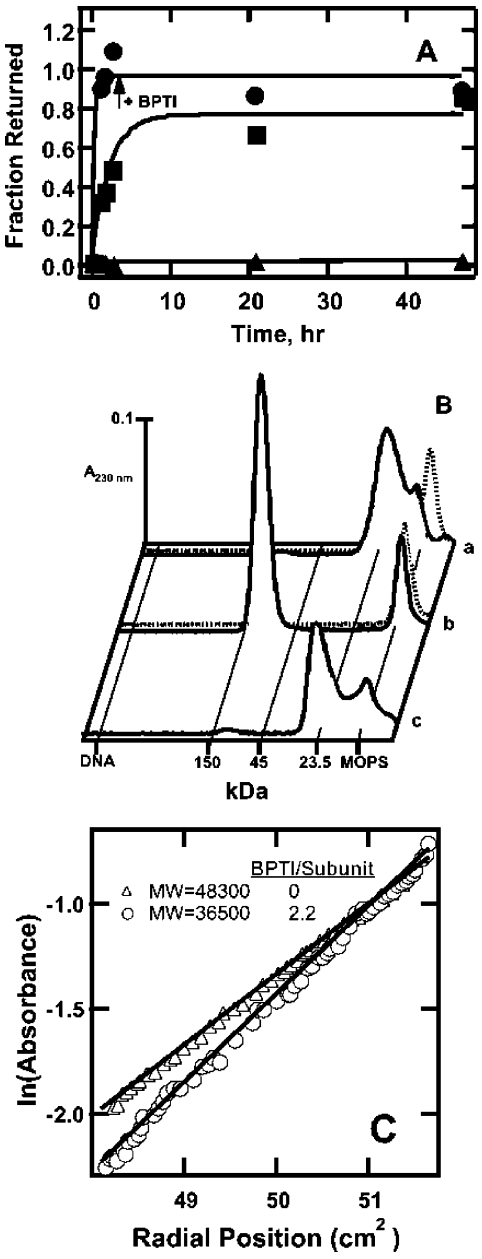

FIGURE 7: The interaction of si-rHTβ with physiological inhibitors BPTI and LBTI. In panel A, reactivation of 8.0 μM si-rHTβ by 0.5 mg/mL heparin was measured in the absence and presence of inhibitors. After decay at 37 °C, si-rHTβ was cooled to 25 °C, and reactivations were performed as follows: addition of heparin followed by addition of BPTI (10.0 μM final) after 100 min (circles); addition of LBTI (8.0 μM final) followed by heparin after 5 min (squares); addition of BPTI (10.0 μM final) followed by heparin after 5 min (triangles). In panel B, SEC analyses were as follows: trace a, 8.0 μM si-rHTβ preincubated with 10.0 μM BPTI for 5 min before addition of heparin (0.5 mg/mL final); trace b, heparin-stabilized rHTβ (0.5 mg/mL heparin final) preincubated with 10.0 μM BPTI for 5 min; trace c, 8 μM si-rHTβ alone. Superimposed on traces a and b is the elution of 10 μM BPTI alone (dotted traces). Elutions were in high salt so that tetramer and monomer could be resolved, and MOPS as a total volume marker was added only to the analysis of si-rHTβ without BPTI, trace c. Panel C is a set of sedimentation equilibrium data at 12000 rpm for 4.5 μM si-rHTβ in the absence and presence of 10 μM BPTI. In the presence of BPTI, a single species with a MW of 36500 (±80) adequately described the data at five different speeds, whereas in the absence of BPTI, a single species was not satisfactory. The MW shown in the absence of BPTI is the weight average for all species that comprise si-rHTβ and is based on linear regression of the data shown in panel C only.

DISCUSSION

Given the high levels of mast cells in connective and mucosal tissues, HTβ is probably one of the most abundant serine proteases found in the body. It also is probably the most biochemically distinct serine protease due to its unusual tetrameric structure and functional instability. Previously, we provided evidence that the functional instability of rHTβ is governed by conformational changes that produce disruption of the S1 pocket (*15*) and destabilization of the tetramer (*14*) as in pathway A of Figure 1. Further support for pathway A is provided in the current study by using small molecule inhibitors that bind primarily to the S1 pocket to stabilize the active conformation of rHTβ. Their use permitted the quaternary structure of rHTβ to be investigated under decay conditions without stabilization by polyanions which have the potential to cross-link subunits. Establishment of pathway A helps to understand the role of heparin in stabilizing HTβ, the structural stability of rHTα, and recent studies reporting a catalytic monomer (*21*, *22*).

Spontaneous Inactivation Follows Pathway A. Controversy over the integrity of the HTβ tetramer as discussed in the introduction led to the proposal of pathways A and B as two possible mechanisms for spontaneous inactivation. Briefly, pathway A postulates that functional instability is a property of the tetramer and that activity loss occurs within the subunits, whereas pathway B postulates that functional instability is a property of the monomer and that the tetramer is primarily the result of solvent influences that promote aggregation to a "pseudotetramer" in which the monomers are stable. The final product of spontaneous inactivation in pathway A is an inactive-destabilized tetramer that dissociates upon dilution, whereas in pathway B it can only be an inactive monomer. Our results support pathway A as subsequently described.

Binding of small competitive inhibitors or complete modification by the small irreversible inhibitor, AEBSF, stabilized the tetramer in decay buffer, indicating that intersubunit contacts are sufficient to maintain the tetramer under physiological conditions in the absence of stabilizing polyanions. Even more definitive was the return of the active tetramer mediated by competitive inhibitors alone at high si-rHTβ concentration (4−5 μM) or by inhibitor plus heparin at low si-rHTβ concentration (0.1 μM). Re-formation of the active tetramer from si-rHTβ where inactive monomer is either the major or the only species would not have occurred unless the tetramer was favored thermodynamically.

The ability of AEBSF modification to stabilize the tetramer is in contrast to that observed with DFP, another small molecule inhibitor that reacts with Ser195. DFP-modified HTβ was shown to dissociate to monomer when incubated at 37 °C for 30 min (*2*) and to retard, but not prevent, structural changes associated with spontaneous inactivation at 25 °C (*14*). The difference in stability is likely related to the size of each inhibitor, with the smaller isopropyl groups of DFP being unable to stabilize the S1 pocket as completely as the larger aminoethylbenzene group of AEBSF.

A link between function and interface stability also was established by limited covalent modification using AEBSF to produce tetramers that contained a mixture of modified and unmodified subunits. The activity of the partially modified tetramers decayed significantly more slowly than unmodified tetramers (Figure 3). The largest decrease in decay rate correlated with a population of unmodified subunits that were in contact with modified subunits at each interface. This result suggests that subunit contacts at both interfaces play a role in maintaining the active conformation and, thus by implication, are weakened by spontaneous inactivation.

The new sedimentation equilibrium studies with rHTβ and si-rHTβ under conditions closer to physiological (0.2 M NaCl) confirm the studies in 1 M NaCl, which showed that the product of spontaneous inactivation was an equilibrium mixture most likely consisting of inactive monomer and inactive tetramer (*14*). For reasons unknown at present, the decay of HTβ from skin used in earlier studies was biphasic with 85% of the activity being lost during a fast phase and the remainder over a much longer time frame (*4*). rHTβ, on the other hand, decays as a single phase (>97% activity loss) such that virtually all species comprising si-rHTβ must arise from the same process (*15*). Most importantly, the equilibrium between the species was demonstrated further by showing its sensitivity to added inhibitors. Addition of leupeptin shifted the si-rHTβ mixture to the tetrameric state (Figure 5) whereas addition of BPTI shifted it to a homogeneous 1:1 protease−inhibitor complex (Figure 7).

Taken together, these findings show that spontaneous inactivation likely involves concerted structural changes that affect, at minimum, the integrity of the S1 pocket and both interfaces. The crystal structure of HTβ (*6*) revealed the S1 pocket in close proximity to the large interface with some residues being common to both. Given this arrangement, a conformational change affecting the S1 pocket is likely to affect the large interface, and vice versa. Less clear is why the small interface is affected.

Stabilization by Heparin. This study is the first to show that small ligands that cannot span subunits have the ability to stabilize and reactivate HTβ in decay buffer. Given this finding, the stabilization of HTβ enzymatic activity by heparin is not due to its ability to bridge and cross-link monomers. Rather, it is more likely that heparin binding favors the active conformation in which intersubunit contacts are inherently strong. Long heparin chains with the ability to bind to multiple sites will bind more strongly than short chains (*34*). This could explain why short heparin or dextran sulfate chains are not as effective as longer chains in stabilizing HTβ activity (*20*).

Our findings are in contrast to recent studies reporting dissociation of the heparin-stabilized tetramer to a heparin-stabilized monomer that is reactive with protein proteolytic inhibitors such as BPTI or SBTI (*21*). Prolonged incubation with BPTI of either heparin-stabilized rHTβ or heparin-reactivated si-rHTβ did not result in a loss of activity, indicating that heparin-stabilized rHTβ is not in equilibrium with a form capable of interacting with BPTI. Moreover, heparin-stabilized rHTβ diluted to subnanomolar concentrations remained sensitive to low concentrations of the divalent inhibitor, CRA-2059, implying little tendency for the heparin-stabilized tetramer to dissociate [this study and previously (*10*)]. Still, dissociation of heparin-stabilized tetramers to monomers that are reactive with BPTI cannot be eliminated as our studies were typically performed under conditions (0.2 M NaCl, pH 6.8) that do not precisely duplicate those reported to favor dissociation (*21*, *22*).

Is a Catalytic Monomer Possible? Although, in our hands, BPTI showed no tendency to react with heparin-stabilized rHTβ, we were able to demonstrate its reaction with si-rHTβ. When added to a reactivation before heparin, BPTI completely blocked the return of active rHTβ by formation of a 1:1 complex with si-rHTβ (Figure 7).

BPTI binds with high affinity to the active site of trypsin-like proteases (e.g., $K_i = 10^{-12}$ M for trypsin) and with less affinity to their zymogen forms (10^{-7} M for trypsinogen) (*33*, *35*, *36*). The weaker binding to trypsinogen is the net result of a portion of the binding free energy being applied to a conformational change that organizes the S1 pocket to accommodate the reactive site Lys residue of the inhibitor. The S1 pocket in the zymogen is nonfunctional because an essential ionic bond between the free amino group of Ile16 and the carboxyl group of Asp194 is not formed.

On the basis of structural parallels between HTβ/si-HTβ with chymotrypsin/chymotrypsinogen, we have speculated that si-rHTβ has a zymogen-like conformation in which the Ile16−Asp194 ionic bond and, in turn, the S1 pocket are disrupted (*14*, *15*). Because the ionic bond disruption/formation is reversible, at least in chymotrypsin (*37*, *38*), interaction of si-rHTβ with BPTI could be mediated via a reorganization of the S1 pocket.

The interaction of BPTI with si-rHTβ raises the possibility that a ligand or protein substrate with sufficient binding energy to reorganize the S1 pocket of si-rHTβ could produce a monomeric HTβ species with catalytic potential, provided that the reassembly of the tetramer is prevented. BPTI binding likely prevents tetramer reassembly by its bulk sterically hindering subunit association. The active monomer reported by Fukuoka and Schwartz (*22*) was produced by the interaction of heparin (5 μM) with dilute si-HTβ (about 5 nM monomer) at pH 6.0. This activity suggests that heparin can interact with si-rHTβ at concentrations too dilute to allow (kinetic or thermodynamic) reassembly of tetrameric species. According to pathway A, this finding would be consistent with the formation a new monomeric species that is not fully equivalent in conformation or catalytic properties to the subunit of the original tetramer. From the kinetic data presented by Fukuoka and Schwartz (*22*), the catalytic activity of their heparin-stabilized monomer was not equivalent to that of a subunit of the original tetramer.

Structure of rHTα. The stabilizing effect of competitive inhibitors on the HTβ tetramer may provide a rationale for the stability of the rHTα tetramer. In contrast to HTβ and rHTβ, rHTα does not catalyze the hydrolysis of substrates but is a stable tetramer under decay conditions displaying the spectral characteristics of active rHTβ (*18*, *39*). On the basis of their crystal structures, the major difference between HTβ and rHTα was in the configuration of the S1 pocket. In the HTβ structure, the S1 pocket was occupied by a competitive inhibitor, and therefore the conformation appeared open and similar to that of bovine trypsin without an inhibitor (*6*). In the rHTα structure, which was crystallized without an inhibitor (*17*), one side of the S1 pocket appeared to have collapsed toward the other, allowing two new electrostatic interactions between residues on opposite sides of the pocket: Lys192 with Glu217 and Asp216 with the oxyanion hole (formed by the amides of Gly193 and Ser195). This collapse effectively fills the S1 pocket, creating a situation somewhat analogous to the binding of a competitive inhibitor. Mutation of Lys192 and Asp216 to the homologous residues in rHTβ (Gln192 and Gly216) converted rHTα to an rHTβ-like protease, suggesting that these electrostatic interactions within the S1 pocket of rHTα were sufficient to stabilize the tetrameric state (*18*). The underlying cause for the unusual S1 pocket structure in rHTα has not been established. It is tempting to speculate that the same forces producing the disruption of the S1 pocket upon spontaneous inactivation of rHTβ also produced the unusual S1 pocket conformation in rHTα. However, in rHTα, the electrostatic interactions limit the extent of change in the S1 pocket, thereby preventing spontaneous inactivation from proceeding to the destabilized tetramer.

Summary. Our data show that active HTβ under decay conditions is a tetramer. Dissociation of the tetramer is a consequence of spontaneous inactivation which produces a destabilized tetramer via concerted structural changes that result in both enzymatic activity loss and a weakening of intersubunit contacts (pathway A). Heparin binding stabilizes the HTβ tetramer by maintaining the structure of subunits in their active conformation, rather than by cross-linking weakly interacting monomers. A monomeric form of HTβ with catalytic potential is possible only after spontaneous inactivation has occurred and requires the interaction of si-rHTβ with a molecule (e.g., protein or heparin) capable of reorganizing the S1 pocket under conditions where reassembly of the tetramer is disfavored.

ACKNOWLEDGMENT

We thank Celera Genomics, Inc., for the kind gift of CRA-2059. We also thank Michael Plotnick for helpful discussions. rHTβ was expressed at the Recombinant Vector and Protein Expression Facility, Wistar Institute, Philadelphia, PA.

REFERENCES

1. Schwartz, L. B., Irani, A.-M. A., Roller, K., Castells, M. C., and Schechter, N. M. (1987) Quantitation of histamine, tryptase, and chymase in dispersed human T and TC mast cells, *J. Immunol. 138*, 2611−2615.
2. Schwartz, L. B., and Bradford, T. R. (1986) Regulation of tryptase from lung mast cells by heparin−stabilization of the active tetramer, *J. Biol. Chem. 261*, 7372−7379.
3. Addington, A. K., and Johnson, D. A. (1996) Inactivation of human lung tryptase: evidence for a re-activatable tetrameric intermediate and active monomers, *Biochemistry 35*, 13511−13518.
4. Schechter, N. M., Eng, G. Y., and McCaslin, D. R. (1993) Human skin tryptase: kinetic characterization of Its spontaneous inactivation, *Biochemistry 32*, 2617−2625.
5. Kozik, A., Potempa, J., and Travis, J. (1998) Spontaneous inactivation of human lung tryptase as probed by size-exclusion chromatography and chemical cross-linking: dissociation of active tetrameric enzyme into inactive monomers is the primary event of the entire process, *Biochim. Biophys. Acta 1385*, 139−148.
6. Pereira, P. J. B., Bergner, A., Macedo-Ribeiro, S., Huber, R., Matschiner, G., Fritz, H., Sommerhoff, C. P., and Bode, W. (1998) Human β-tryptase is a ring-like tetramer with active sites facing a central pore, *Nature 392*, 306−311.
7. Smith, T. J., Houghland, M. W., and Johnson, D. A. (1984) Human lung tryptase−purification and characterization, *J. Biol. Chem. 259*, 11046−11051.
8. Harvima, I. T., Schechter, N. M., Harvima, R. J., and Fräki, J. E. (1988) Human skin tryptase: purification, partial characterization and comparison with human lung tryptase, *Biochim. Biophys. Acta 957*, 71−80.
9. Alter, S. C., Kramps, J. A., Janoff, A., and Schwartz, L. B. (1990) Interactions of human mast cell tryptase with biological protease inhibitors, *Arch. Biochem. Biophys. 276*, 26−31.

10. Selwood, T., Elrod, K. C., and Schechter, N. M. (2003) Potent bivalent inhibition of human tryptase-β by a synthetic inhibitor, *Biol. Chem. 384*, 1605−1611.
11. Fiorucci, L., and Ascoli, F. (2004) Mast cell tryptase, still an enigmatic enzyme, *Cell. Mol. Life Sci. 61*, 1278−1295.
12. Schwartz, L. B. (1994) Tryptase: a mast cell serine proteinase, *Methods Enzymol. 244*, 88−100.
13. Schwartz, L. B., Bradford, T. R., Douglas, C. L., and Chlebowski, J. F. (1990) Immunologic and physiochemical evidence for conformational changes occurring on conversion of human mast cell tryptase from active tetramer to inactive monomer—production of monoclonal antibodies recorgnizing active tryptase, *J. Biol. Chem. 144*, 2304−2311.
14. Schechter, N. M., Eng, G. Y., Selwood, T., and McCaslin, D. R. (1995) Stuctural changes associated with the spontaneous inactivation of the serine proteinase human tryptase, *Biochemistry 34*, 10628−10638.
15. Selwood, T., McCaslin, D. R., and Schechter, N. M. (1998) Spontaneous inactivation of human tryptase involves conformational changes consistent with conversion of the active site to a zymogen-like structure, *Biochemistry 37*, 13174−13183.
16. Ren, S., Sakai, K., and Schwartz, L. B. (1998) Regulation of human mast cell β-tryptase: conversion of inactive monomer to active tetramer at acid pH, *J. Immunol. 1998*, 4561−4569.
17. Marquardt, U., Zettl, F., Huber, R., Bode, W., and Sommerhoff, C. (2002) The crystal structure of human α1-tryptase reveals a blocked substrate-binding region, *J. Mol. Biol. 321*, 491−502.
18. Selwood, T., Wang, Z.-M., McCaslin, D. R., and Schechter, N. M. (2002) Diverse stability and catalytic properties of human tryptase α and β isoforms are mediated by residue differences at the S1 pocket, *Biochemistry 41*, 3329−3340.
19. Sommerhoff, C. P., Bode, W., Pereira, P. J., Stubbs, M. T., Sturzebecher, J., Piechottka, G. P., Matschiner, G., and Bergner, A. (1999) The structure of the human βII-tryptase tetramer: fo(u)r better or worse, *Proc. Natl. Acad. Sci. U.S.A. 96*, 10984−10991.
20. Alter, S. C., Metcalfe, D. D., Bradford, T. R., and Schwartz, L. B. (1987) Regulation of human mast cell tryptase: effects of enzyme concentration, ionic strength and negative charge density, *Biochem. J. 248*, 821−827.
21. Fajardo, I., and Pejler, G. (2003) Formation of active monomers from tetrameric human β-tryptase, *Biochem. J. 369*, 603−610.
22. Fukuoka, Y., and Schwartz, L. B. (2004) Human β-tryptase: detection and characterization of the active monomer and prevention of tetramer reconstitution by protease inhibitors, *Biochemistry 43*, 10757−10764.
23. Wang, Z.-M., Walter, M., Selwood, T., Rubin, H., and Schechter, N. M. (1998) Recombinant expression of human mast cell proteases chymase and tryptase, *Biol. Chem. 379*, 167−174.
24. Evans, S. A., Olson, S. T., and Shore, J. D. (1982) *p*-Aminobenzamidine as a fluorescent probe for the active site of serine proteases, *J. Biol. Chem. 257*, 3014−3017.
25. Schultz, R. M., Varma-Nelson, P., Ortiz, R., Kozlowski, K. A., Orawski, A. T., Pagast, P., and Frankfater, A. (1989) Active and inactive forms of the transition state analog protease inhibitor leupeptin: explanation of the observed slow binding of leupeptin to cathepsin B and papain, *J. Biol. Chem. 264*, 1497−1507.
26. Citron, M., Diehl, T. S., Capell, A., Haass, C., Teplow, D. B., and Selkoe, D. J. (1996) Inhibition of amyloid beta-protein production in neural cells by the serine protease inhibitor AEBSF, *Neuron 17*, 171−179.
27. Markwardt, F., Hoffmann, J., and Körbs, E. (1973) The influence of synthetic thrombin inhibitors on the thrombin-antithrombin reaction, *Thromb. Res. 2*, 343−348.
28. Ohkubo, I., Huang, K., Ochiai, Y., Takagaki, M., and Kani, K. (1994) Dipeptidyl peptidase IV from porcine seminal plasma: purification, characterization, and N-terminal amino acid sequence, *J. Biochem. 116*, 1182−1186.
29. Fritz, H., and Wunderer, G. (1983) Biochemistry and applications of aprotinin, the kallikrein inhibitor from bovine organs, *Arzneim.-Forsch./Drug Res. 33*, 479−494.
30. Kassell, B. (1970) Bovine trypsin-kallikrein inhibitor (kunitz inhibitor, basic pancreatic trypsin inhibitor, polyvalent inhibitor from bovine organs), *Methods Enzymol. 19*, 844−852.
31. Castro, M. J. M., and Anderson, S. (1996) Alanine point-mutations in the reactive region of bovine pancreatic trypsin inhibitor: effects on the kinetics and thermodynamics of binding to β-trypsin and α-chymotrypsin, *Biochemistry 35*, 11435−11446.
32. Quast, U., Engel, J., Heumann, H., Krause, G., and Steffen, E. (1974) Kinetics of the interaction of bovine pancreatic trypsin inhibitor (kunitz) with α-chymotrypsin, *Biochemistry 13*, 2512−2520.
33. Laskowski, M., Jr., and Kato, I. (1980) Protein inhibitors of proteinases, *Annu. Rev. Biochem. 49*, 593−626.
34. Mammen, M., Choi, S.-K., and Whitesides, G. M. (1998) Polyvalent interaction in biological systems: implications for the design and use of multivalent ligands and inhibitors, *Angew. Chem., Int. Ed. 37*, 2755−2794.
35. Bode, W., Schwager, P., and Huber, R. (1978) The transition of bovine trypsinogen to a trypsin-like state upon strong ligand binding. The refined crystal structures of the bovine trypsinogen-pancreatic trypsin inhibitor complex and its ternary complex with Ile-Val at 1.9 Å resolution, *J. Mol. Biol. 118*, 99−112.
36. Bode, W. (1979) The transition of bovine trypsinogen to a trypsin-like state upon strong ligand binding, II. The binding of the pancreatic trypsin inhibitor and of isoleucine-valine and of sequentially related peptides to trypsinogen and to *p*-guanidinobenzoate-trypsinogen, *J. Mol. Biol. 127*, 357−374.
37. Fersht, A. R., and Requena, Y. (1971) Equilibrium and rate constants for the interconversion of two conformations of α-chymotrypsin: the existence of a catalytically inactive conformation at neutral pH, *J. Mol. Biol. 60*, 279−290.
38. Fersht, A. R. (1972) Conformational equilibria in α- and δ-chymotrypsin: the energetics and importance of the salt bridge, *J. Mol. Biol. 64*, 497−509.
39. Huang, C., Li, L., Krilis, S. A., Chanasyk, K., Tang, Y., Li, Z., Hunt, J. E., and Stevens, R. L. (1999) Human tryptases α and β/II are functionally distinct due, in part, to a single amino acid in one of the surface loops that forms the substrate-binding cleft, *J. Biol. Chem. 274*, 19670−19676.

BI047765U